Paper 138

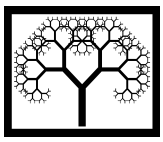

Proceedings of the Tenth International Conference
on Computational Structures Technology,
B.H.V. Topping, J.M. Adam, F.J. Pallarés,
R. Bru and M.L. Romero, (Editors),
Civil-Comp Press, Stirlingshire, Scotland

The "Rognosa" Tower in San Gimignano: Digital Acquisition and Structural Analysis

M. Callieri[1], M. Corsini[1], M. Girardi[2], C. Padovani[2], A. Pagni[2], G. Pasquinelli[2] and R. Scopigno[1]
[1] Visual Computing Laboratory
[2] Mechanics of Materials and Structures Laboratory
Information Science and Technologies Institute "A. Faedo"
ISTI-CNR, Pisa, Italy

Abstract

The paper describes the research activities conducted on the 13th century Rognosa tower in San Gimignano (Siena, Italy), the historic town inscribed on the Unesco World Heritage List in 1990. A structural nonlinear analysis of the tower has been performed via the freeware finite element code NOSA. The finite element mesh of the tower has been generated using a three-dimensional digital model of the tower and the surrounding buildings. The geometry data has been acquired by means of a time-of-flight laser scanner and then processed into the open source software MeshLab and other geometry processing tools. The behaviour of the tower, subjected to its own weight and time-dependent loads modelling the seismic excitations, has been investigated.

Keywords: masonry towers, numerical modelling, finite element method, masonry-like materials, nonlinear dynamics, three-dimensional scanning, geometry processing.

1 Introduction

The assessment of monumental buildings involves performing a series of operations requiring various types of expertise and technologies. The St@rt project (Sciences and Technologies for the Artistic, Architectural and Archaeological Tuscan heritage), funded by the region of Tuscany (Italy) for the three year period 2007-2010, aims to integrate different research and civil services skills in the field of cultural heritage. The project's activities have focused on the Rognosa tower in San Gimignano, chosen as case study to test the technologies and procedures developed by the partners.

The San Gimignano Rognosa tower, built during the 13th century, is one of the historic centre's most ancient and best preserved. The tower, including its bell chamber, is about 52 m high with respect to ground level. The outer dimensions of

the tower's horizontal section are about (8x6) m, and the walls are about 2 m thick, with little or no variation along their height. In keeping with the traditional construction techniques used in San Gimignano's towers, each wall is made up of an inner and an outer layer of lime stone, the intermediate part being made of a very cohesive mortar core. The tower's horizontal floors are constituted by masonry vaults for the first four levels, while the upper floors are wooden. The lowest about 19 m of the tower's height are surrounded by other buildings, whose roofs are made of flexible wooden and iron structures. At level +8.6 m the tower is embedded within a system of massive masonry vaults, which constitute the main floor of the ancient Leggieri Theatre and are partially visible from the square (see Fig. 1-3). The lower part of the tower is characterized by some openings providing access from the surrounding buildings, while the upper part seems to be quite monolithic, with only a few small openings. In correspondence to the lowest opening, at about 4 m above the level of the square, a restriction of the tower's section wall is visible, where one flight of the staircase built on the tower's external surface has been carved directly into the tower's wall. A first visual inspection of the tower did not reveal visible cracked zones.

The study described in this paper stems from the collaboration between the Mechanics of Materials and Structures Laboratory (MMS Lab) and the Visual Computing Laboratory (VC Lab) of the Information Science and Technologies Institute (ISTI) of CNR, within the framework of the aforementioned St@rt project. The collaboration aims to develop procedures for combining visual computing and computational mechanics technologies to obtain realistic models of monumental structures in complex architectural contexts.

2 Digital acquisition

2.1 3D Geometry Acquisition

The geometry of the external surface of the Rognosa tower and of the surrounding buildings has been acquired by means of a RIEGL LMS-Z390i time-of-flight (TOF) laser scanner. Such devices work by emitting a laser impulse along a specific direction and recording the time interval between emission and the appearance of the laser spot on the surface to be measured. The measurement is iterated along a polar grid, thus covering the entire area of interest. The obtainable precision is about 3-5 mm.

Planning and carrying out 3D acquisition of the Rognosa tower's geometry was complicated by the fact that the tower emerges from the rooftops of some very large buildings all round (see Fig. 1). However, thanks to the cooperation of the San Gimignano Township Engineering Office, the necessary permits have been obtained to exploit various viewpoints from private homes and commercial buildings surrounding the tower.

The tower's surface has therefore been acquired from four different position, each selected to provide the best possible coverage of one side and, at the same time, a good view of another adjacent side, in order to facilitate the alignment process and

provide coverage of all details from multiple angles. Additional scans were carried out to acquire the facade of the building encompassing the tower and the front arcade overlooking the square, where a portion of the tower's base is visible. Unfortunately, acquisition of the tower's inside geometry is made impossible by the fact that it is only accessible via a wall stair and the view of its highest portion from the lowest is partially hidden by wooden floors. Thus, a series of classical measurements has been performed to obtain the missing geometric information.

Redundant scanning is essential when a triangulated model is needed. For this reason, each scan was carried out at a higher resolution than that used in "common" practice, and each part of the tower was carefully covered from multiple points of view. High redundancy was used in the processes of both alignment (to provide strict and precise alignment), and merging (to reduce intrinsic sampling noise).

The resulting resolution of each scan varies quite widely, even within a single map. In fact, the lower part of the tower structure has a higher resolution than the top and the "straighter" face in each scan has a higher density than the "less straight" one. Nevertheless, thanks to the high sampling rate of each scan, the final result has provided a high quality reconstruction, with a mean resolution of about 5 mm and quite uniform coverage in terms of point density.

The total time required for the acquisition was roughly 6 hours, which actually represents quite a long time for such a structure. Most of this time was spent moving from one scanning position to another. Once the instrumentation was set up, each full scan consisted of a 2 minute overview scan (low resolution, 360 degree acquisition) followed by a 15-20 minute high resolution scan of some selected areas.

2.2 Data Processing

2.2.1 Data importing

Time-of-flight scanners are commonly used for surveying buildings, work sites and architectural complexes. In most cases, the output required is a point cloud obtained by superimposing the aligned range scans.

However, for the specific purposes of the project, the ideal representation is a triangulated surface, which is more compact, easier to manage at rendering time and provides more complete information about surface features.

A preliminary step to producing a triangulated surface is to convert each scan to a more suitable data format. Since the software driving TOF scanners typically does not provide good means for range scan triangulation and data exportation, some custom converters have been implemented by the VC Lab to transfer the data from the RIEGL proprietary format to a more open standard, in our case, PLY. Each map was then manually purged of false points (spikes due to sampling errors, "floating" points caused by reflections) and extraneous elements (birds and caper plants on the tower's surface).

No filtering has been applied to the data. In fact, thanks to the redundancy employed, the merging process has been able to reduce sampling noise without using any smoothing algorithm at all.

Figure 1. Acquisition of the tower's geometry by means of a TOF laser scanner.

The entire step of processing the range maps, generating the 3D model and extracting the measurements was carried out using software developed by the VC Lab [1, 2]. This software is based on state-of-the-art algorithms for processing scanned 3D data, and can efficiently manage huge amounts of data.

2.2.1 Alignment

The alignment process consists of bringing each range scan from the local to a common reference system.

In most cases, alignment among scans is achieved by using markers positioned on the building to be acquired, even exploiting the support of a total station. In this case, however, placing the markers on the tower surface would have been very difficult. Alignment was then achieved by using the redundancy of the acquired geometric data. In a first step, the scans are put close one to another by using some corresponding points marked by the user. This first rough alignment enables the software to produce a millimetre-precise alignment using the Iterative Closest Point (ICP) algorithm [3].

The vertical axis of the model has been aligned with the local direction of gravity acceleration: a single scan acquired with the scanner in a straight position is sufficient to correctly orient the vertical axis of the model. The origin and the orientation of the other axes were then chosen in such a way as to simplify management of the model (for both the rendering and its use in the structural analysis tool).

2.2.1 Model generation

After having aligned all the range scans in a common reference frame, one further step is necessary to obtain a triangulated surface from the various range scans; this is commonly referred to as merging.

The VC Lab tools for surface merging in a volumetric space work by dividing the volume of the object into small cells and trying to find the surface that best approximates the sampled points in each cell. Then, each cell is triangulated using the marching cubes algorithm [4, 5], so that adjacent cells exhibit coherent triangulation. This approach is especially useful to cope with noisy input data, as in the current case. An out-of-core memory management strategy aids in the processing of large datasets, there by allowing the user to produce very complex 3D surfaces using a normal PC.

The merging resolution for the current case was set to 1 centimetre, even if the resolution of the starting data was higher. Setting a lower resolution for the reconstruction step helps cleaning the resulting model of sampling noise. The merging process for the tower data lasted 3 hours.

The model thus obtained was composed of 28 million triangular faces. A first cleaning step reduced this dataset to 18 million elements, and smaller working models (10, 6, 4, 2 millions triangles) have also been produced for the various aims of the project. The measure extraction has been carried out on the 10 million elements model, while the 4 million elements model has been used for rendering and the presentations (see Fig. 2).

2.3 Measures Extraction

The 3D model generated by the VC Lab has been used by the MMS Lab to extract geometry information for constructing the finite element model of the tower. The tower's external geometry has been acquired by extracting some cross sections from the 3D model by means of MeshLab (http://meshlab.sourceforge.net) [2], an open source tool developed by the VC Lab.

Extracting a section from a triangulated surface usually produces very complex polylines, but their complexity can be easily brought to the desired resolution. The model sections have been produced as follows:

- 16 Horizontal (X-Y plane) sections, one every 2 meters for the entire height of the tower external to the adjacent buildings;
- 4 Vertical (Z-X plane) sections;
- 4 Vertical (Z-Y plane) sections;

The sections have been exported in DXF file format and imported into the pre-processing software.

Other information on various details of the tower's surface, such as the openings and the bell chamber, have been obtained by picking some measures directly on the 3D model. MeshLab, in fact, implements a very useful feature to select specific points on the 3D model and export their coordinates in ASCII format. In this way the contour of each geometric element of the model can be easily traced.

MeshLab also enables acquiring information on the mean inclination of each side of the tower as well as on the local deviation of the external surface from the gravity direction.

The accuracy of the 3D model has also allowed highlighting some interesting architectonical details, such as a restriction in the tower's external contur of about 20 mm, clearly visible in the highest part of the structure.

Figure 2. 3D model of the Rognosa tower and the Cathedral Square.

3 Structural analysis

Although masonry towers represent an important part of the world's ancient architectonic heritage, their mechanical behaviour is not well known yet. In fact, their response to dynamic actions is nonlinear and heavily dependent on the construction techniques utilised. Moreover, they are characterized, even in the static case, by high compressive stresses that can cause additional damage in correspondence to openings or other geometrical irregularities. Even though some general aspects can be highlighted via simplified linear [6 - 9] and nonlinear [10,11] models, careful acquisition of the geometry as well as the use of more refined mechanical models are of great importance [12].
The following described an analysis of the static and dynamic behaviour of the Rognosa tower performed via the finite element code NOSA [13], a freeware software for nonlinear analyses developed by the MMS Lab (http://www.isti.cnr.it/comesnosa/).

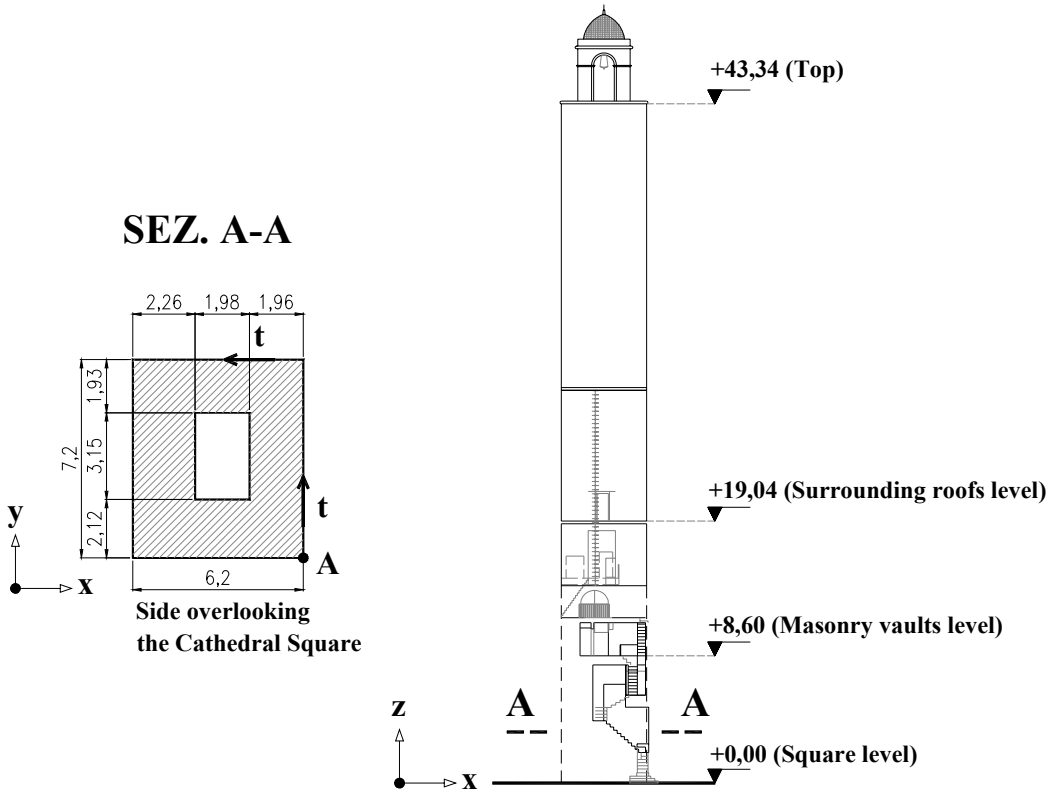

Figure 3. The Rognosa tower: base cross section and vertical view.
(Geometric survey by Studio F. Titoni).

3.1 The numerical method

The constitutive model and numerical techniques for solving the static and dynamic problems of masonry constructions implemented in the NOSA code are described in [13] and [14]. In order to model the behaviour of masonry constructions, we use the constitutive equation of masonry-like materials with bounded compressive strength. Masonry is assumed to be a nonlinear hyperelastic material with Young's modulus $E > 0$, Poisson ratio ν, where $0 \le \nu < 1/2$, and maximum compressive stress $\sigma_0 < 0$. We denote by *Sym* the vector space of symmetric tensors equipped with the scalar product $\mathbf{A} \cdot \mathbf{B} = tr(\mathbf{AB})$, with $\mathbf{A}, \mathbf{B} \in Sym$ and *tr* the trace. Sym^- and Sym^+ are the subsets of *Sym* constituted by the negative and positive semidefinite tensors, respectively. We assume that the infinitesimal strain $\mathbf{E} \in Sym$ is the sum of an elastic part $\mathbf{E}^e \in Sym$ and two mutually orthogonal inelastic parts $\mathbf{E}^f \in Sym^+$ and $\mathbf{E}^c \in Sym^-$, respectively called fracture strain and crushing strain,

$$\mathbf{E} = \mathbf{E}^e + \mathbf{E}^f + \mathbf{E}^c,\ \mathbf{E}^f \cdot \mathbf{E}^c = 0. \tag{1}$$

We moreover assume that the Cauchy stress **T** depends linearly and isotropically on $\mathbf{E}^e$,

$$\mathbf{T} = \frac{E}{1+\nu}[\mathbf{E}^e + \frac{\nu}{1-2\nu} tr(\mathbf{E}^e)\mathbf{I}], \tag{2}$$

with $\mathbf{I} \in Sym$ the identity tensor. Lastly, we assume that **T**, $\mathbf{E}^f$ and $\mathbf{E}^c$ satisfy the conditions

$$\mathbf{T} \in Sym^-, \quad \mathbf{T} - \sigma_0 \mathbf{I} \in Sym^+, \tag{3}$$

$$\mathbf{E}^f \cdot \mathbf{T} = (\mathbf{T} - \sigma_0 \mathbf{I}) \cdot \mathbf{E}^c = 0. \tag{4}$$

By using the coaxiality of **E**, **T**, $\mathbf{E}^f$ and $\mathbf{E}^c$, the stress tensor **T** satisfying the constitutive equation (1)-(4) can be expressed as a nonlinear function of the total strain **E**, $\mathbf{T} = \hat{\mathbf{T}}(\mathbf{E})$. The explicit expression for $\mathbf{T} = \hat{\mathbf{T}}(\mathbf{E})$ can be found in [13], together with its derivative $D_E\hat{\mathbf{T}}(\mathbf{E})$ with respect to **E**.

The static and dynamic problems of masonry shell structures, such as vaults, domes and towers are solved by using quadrilateral eight-node shell elements based on the Love-Kirchhoff hypothesis [15, 16].

The dynamic problem of masonry bodies is treated in [17] where the existence and uniqueness of the solution to the mixed problem are dealt with. In [14] a numerical procedure is proposed with the aim of solving the dynamic problem of masonry structures via the finite-element method. The equation of the motion is integrated

directly, that is, we perform the time integration of the system of ordinary differential equations obtained by discretising the structure into finite elements. In particular, at each time step, a system of the type

$$K(u_t)\Delta u + C\Delta\dot{u} + M\Delta\ddot{u} = \Delta f \qquad (5)$$

is solved via the Newmark method. In Equation (5) u_t is the vector of nodal displacements at time t, Δf is the load increment, and Δu, $\Delta\dot{u}$ and $\Delta\ddot{u}$ are respectively the incremental nodal displacements, velocities and accelerations. K, C and M are the stiffness, damping and mass matrices of the structure, respectively. In agreement with Rayleigh's assumption, we have $C = \alpha M + \beta K$, where α and β are constants to be determined from the vibration frequencies of the structure regarded as linear elastic and from the corresponding damping ratios [18]. Moreover, the Newton-Raphson algorithm is applied to solve the nonlinear algebraic system obtained from Equation (5) via the Newmark method, and the tangent stiffness matrix is calculated using the explicit expression of $D_E\hat{\mathbf{T}}(\mathbf{E})$.

The Rognosa tower has thus been analysed using the NOSA code with the aim of assessing its static behaviour and seismic vulnerability. The structural model of the tower still suffers from some uncertainties regarding the thickness and mechanical properties of each of the layers constituting the walls, the shape and depth of the foundations and the real constraints imposed on the tower by the surrounding structures. Experimental tests on the tower are still under way, so we have adopted values commonly used in the literature for the elastic modulus and the density of the walls. The presence of the surroundings structures has therefore been simulated in terms of loads and masses applied at level + 8.6 m (for those regarding the masonry vaults overlooking the Square and the main floor of the Leggieri Theatre) and at level +19.04 m for the roofs surrounding the tower (see also Figure 3). Instead, the kinematic constraints have been applied only at the level of the Cathedral Square, in order to simulate a base clamped structure.

The tower has been discretised into 6477 shell elements. We have assumed E = 5000 MPa, ν=0.2, $\sigma_0 = -3$ MPa and γ = 2000 kg/m^3 for the mass density. The damping effects are modelled by using the values α = 0.0989673 s^{-1}, β = 0.00400879 s, calculated for a damping ratio ξ = 2%. The structure has been subjected first to gravity loads and then to a seismic acceleration applied at the base. We denote by T_{zz}, E^f_{zz} and E^c_{zz} the normal stress and the fracture and crushing components of the strains in the z direction, repectively, and by E^f_{tt} the component of the fracture strains in the direction t indicated in Figure 3; u_x is the component of displacement u along x.

3.2 Static analysis

A static analysis has been performed by considering the tower to be subjected to its own weight and to vertical loads that take into account the presence of the surrounding buildings. Figures 4 and 5 show the distribution of the stress T_{zz} and

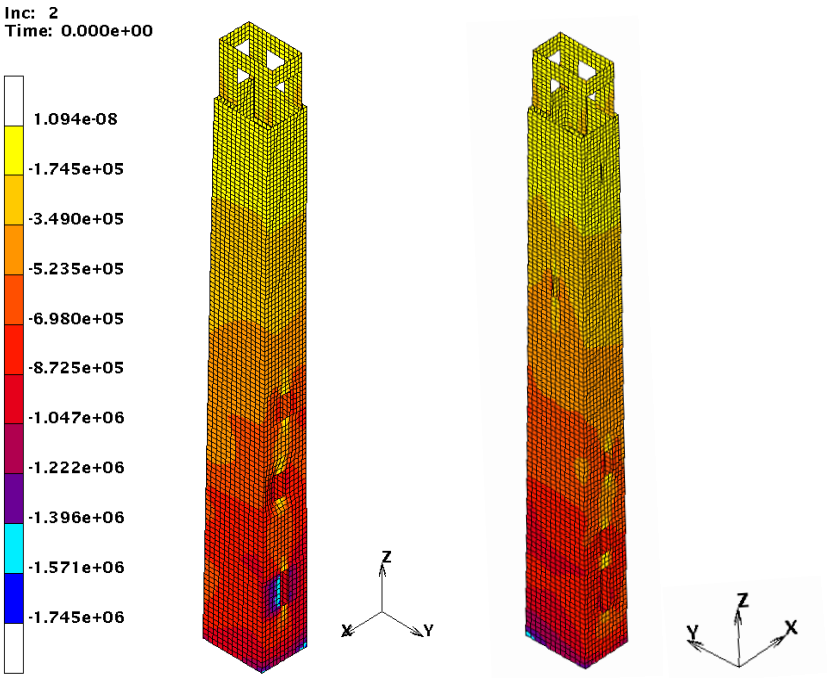

Figure 4. Static analysis: distribution of the stress T_{zz} on the external surface of the Tower for vertical loads (stresses in Pa).

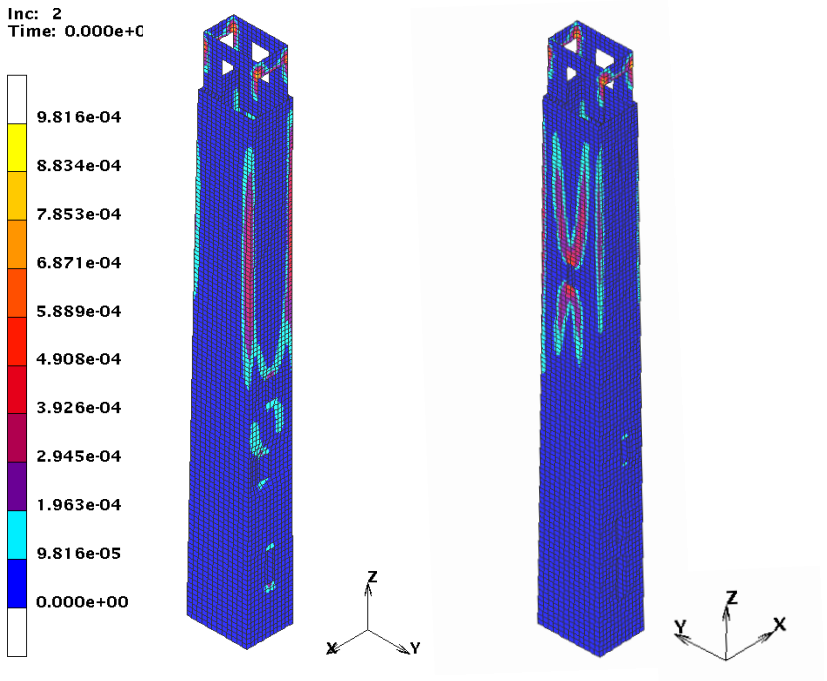

Figure 5. Static analysis: distribution of the crack strain E^f_{tt} on the external surface of the Tower for vertical loads.

the fracture strain E^f_{tt}, respectively. Due to the eccentricity of the external loads, the highest compression values are reached at the corners of the base section, but because these values are always lower than σ_0, no crushing damage is detected in the tower. The greatest values of the fracture strains reveal to be in correspondence to the openings and in the highest part of the bell chamber. Additional damage can be observed in the upper part of the tower, in correspondence to the section's corners - probably due to the absence of effective horizontal diaphragms - and near the tower's base, in correspondence to the section's restriction described in the Introduction.

3.3 Dynamic analysis

After the static analysis, the tower was subjected to the horizontal component of the Nocera Umbra earthquake of 1997 (in the x direction). The Nocera Umbra earthquake lasted 41.30 s and generated a maximum acceleration (PGA) of 4.3192 m/s^2. Figure 6 shows a plot of the ground acceleration for the first 15 seconds. We have used a time step of 10^{-2} s and performed two analyses: the former considering the tower to be made of a linear elastic material, the latter considering a masonry-like material with constitutive equation (1)-(4).

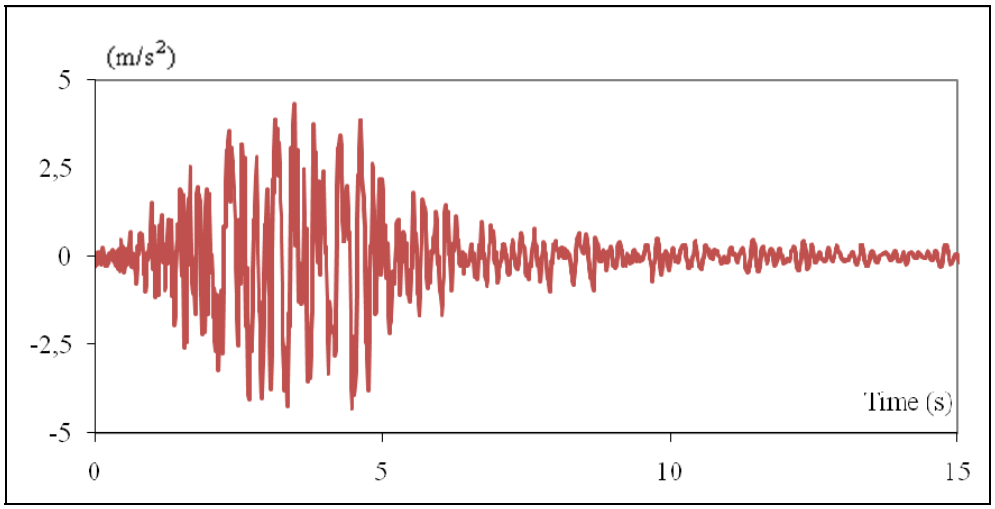

Figure 6. Accelerogram of the Nocera Umbra earthquake, 1997.

Figures 7, 8 and 9 show the distribution of T_{zz}, E^c_{zz} and E^f_{zz} on the external surface of the tower at time t = 3.41 s, when these quantities reach the critical value. Again, the maximum crashing damage is recognized at the tower's base, while the maximum values of the fracture strain tensor are reached in the highest part of the tower, focused near the openings and in correspondence to the bell chamber. Figures 10 to 12 show the time-history of T_{zz}, E^c_{zz} and E^f_{zz} for point A, at the base section's corner (see Figure 3). In particular, Figure 10 highlights the differences between the linear elastic and the masonry-like behaviour.

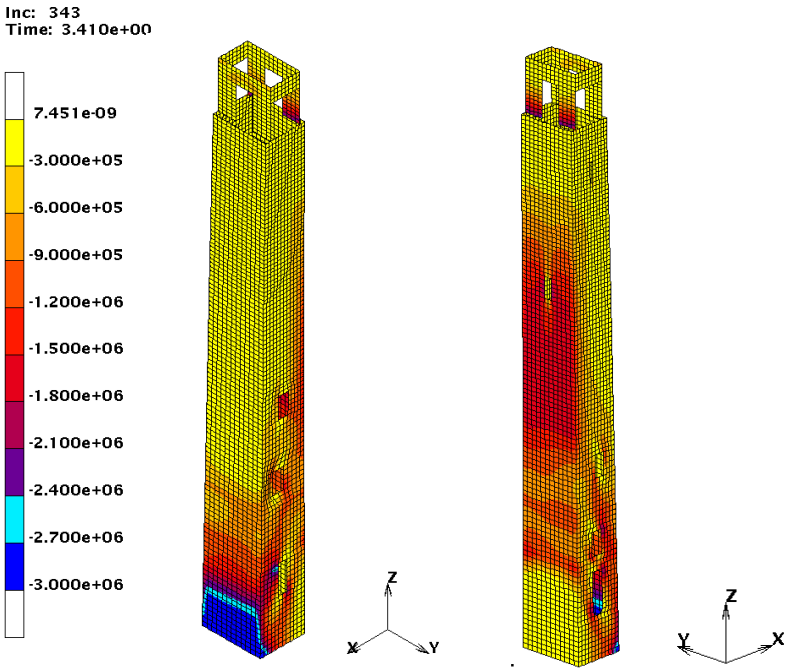

Figure 7. Dynamic analysis: distribution of the stress T_{zz} on the external surface of the Tower at time 3.41s (stresses in Pa).

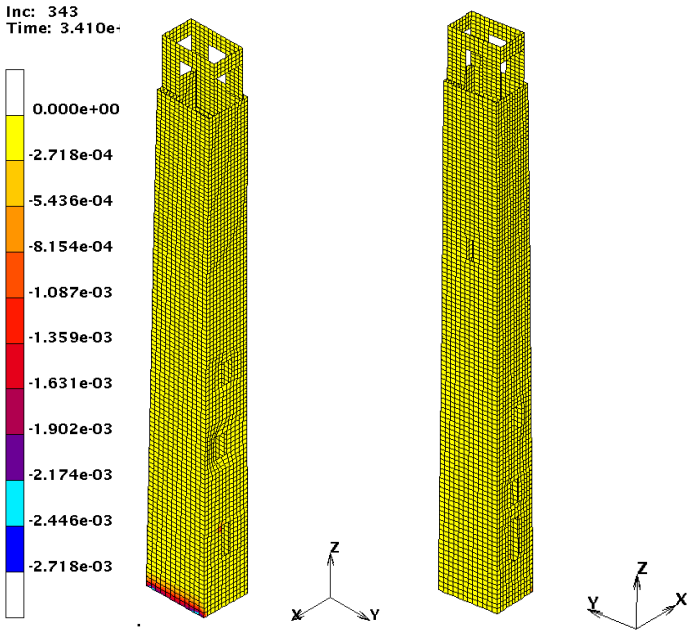

Figure 8. Dynamic analysis: distribution of the crushing strain $E^c{}_{zz}$ on the external surface of the Tower at time 3.41 s.

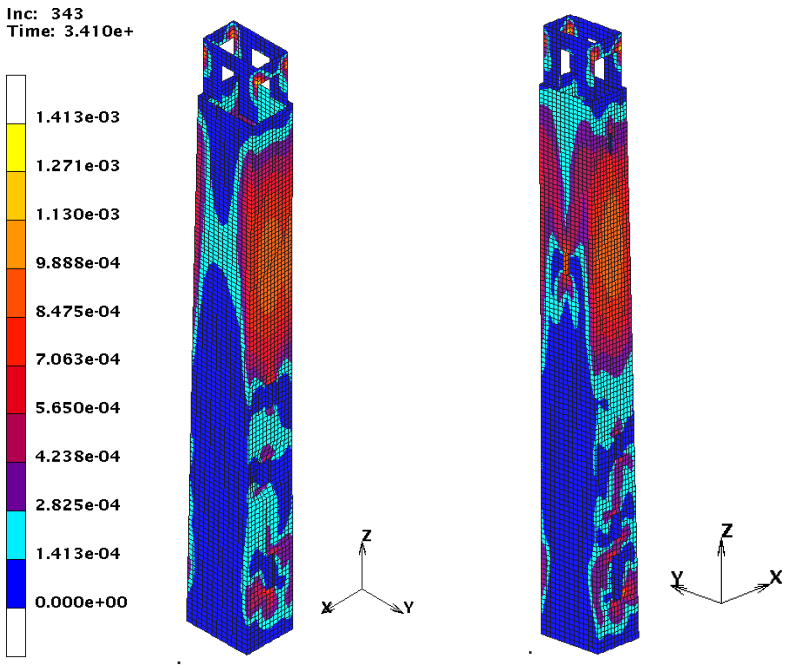

Figure 9. Dynamic analysis: distribution of the crack strain E^f_{tt} on the external surface of the Tower at time 3.41 s.

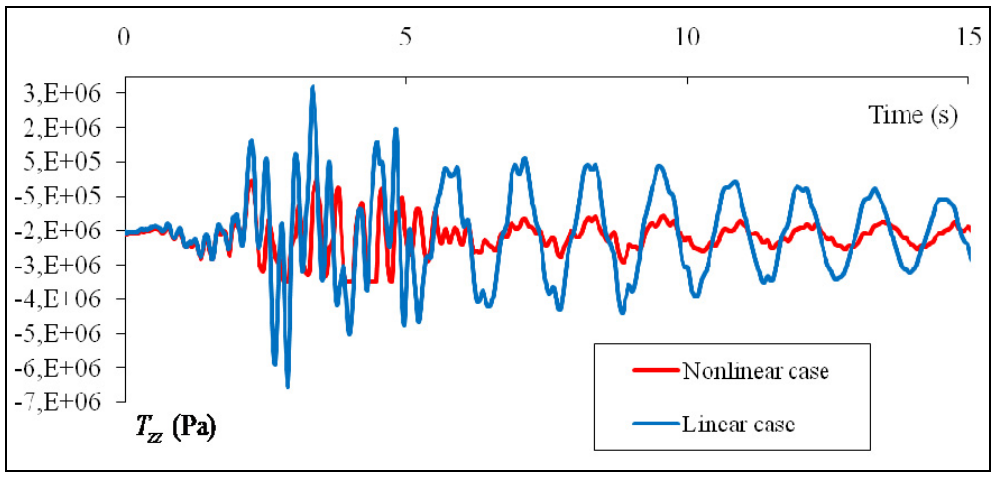

Figure 10. Stress T_{zz} vs. time at point A.

Bell towers typically exhibit a certain vulnerability in correspondence to the bell chamber, which is the structure's highest element and is usually built separately from the rest of tower's structure. Figures 13 to 15 show the behaviour of the bell chamber pillars of the Rognosa tower during the earthquake. In particular, figures 14 and 15 show that the pillars exhibit typical bending behaviour, with a marked difference between the linear and the nonlinear case and high values of the fracture

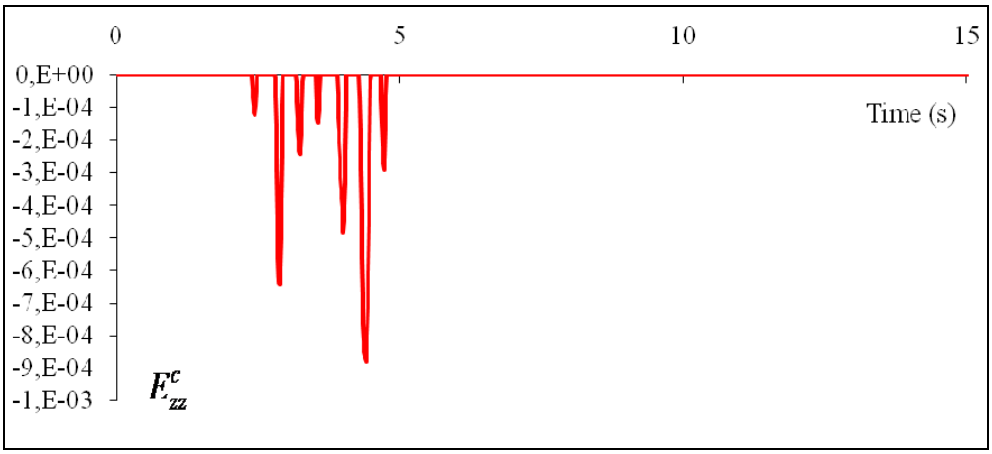

Figure 11. Crushing strain E^c_{zz} vs. time at point A.

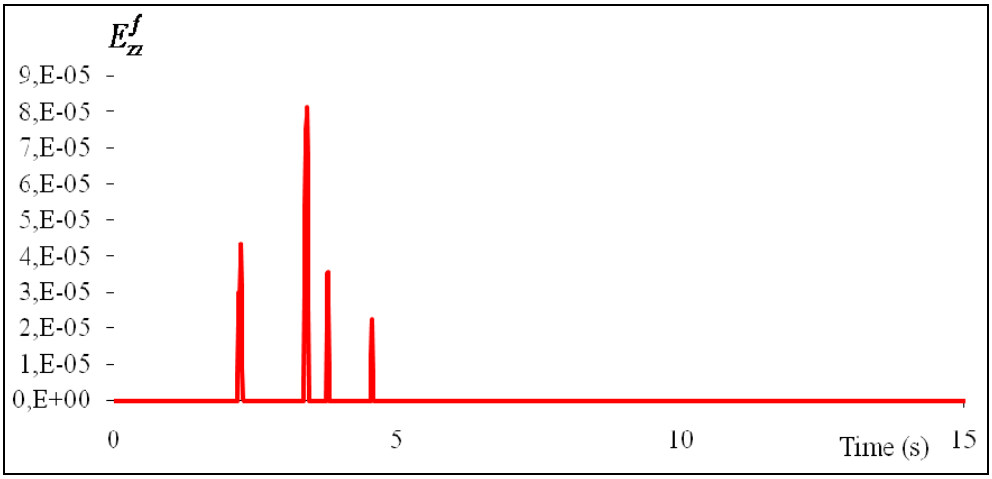

Figure 12. Fracture strain E^f_{zz} vs. time at point A.

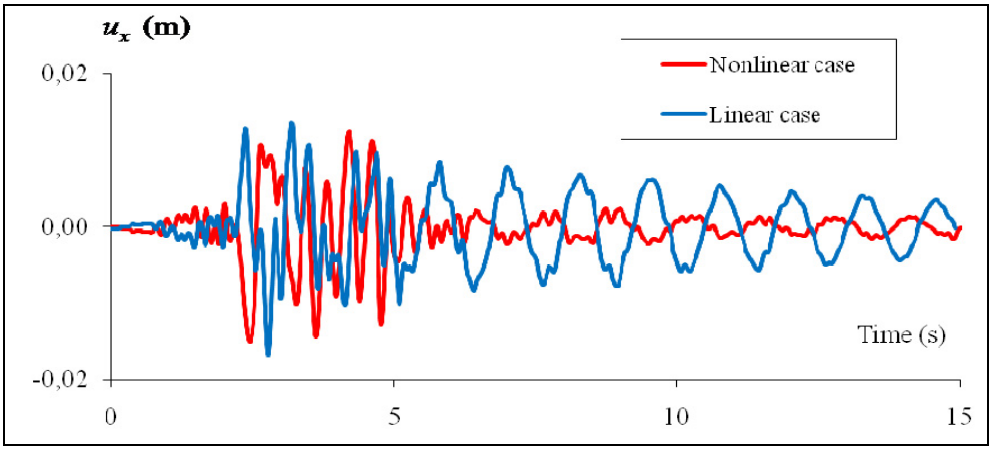

Figure 13. Relative x-displacement u_x of the top of the bell chamber (node 18805) with respect to the top of the tower (node 18253) vs. time.

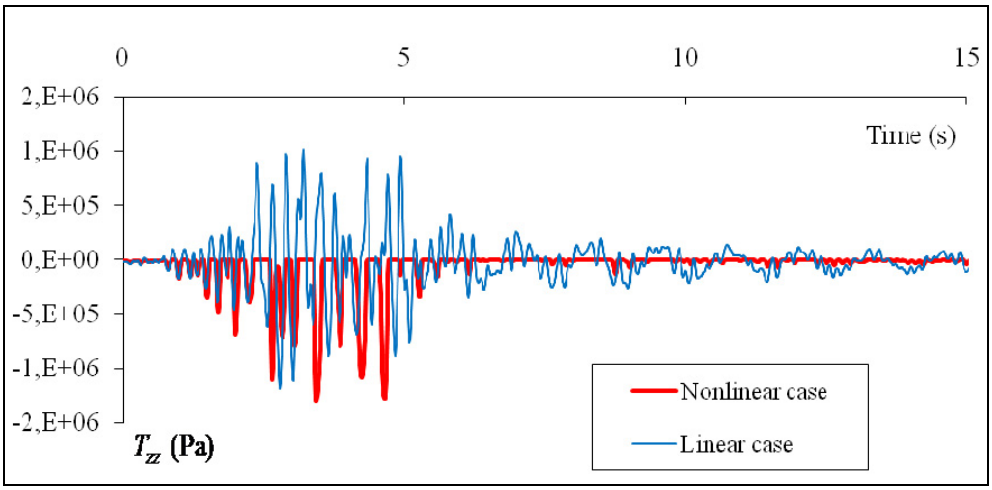

Figure 14. Stress T_{zz} vs. time at the base of a bell chamber's pillar (node 18253).

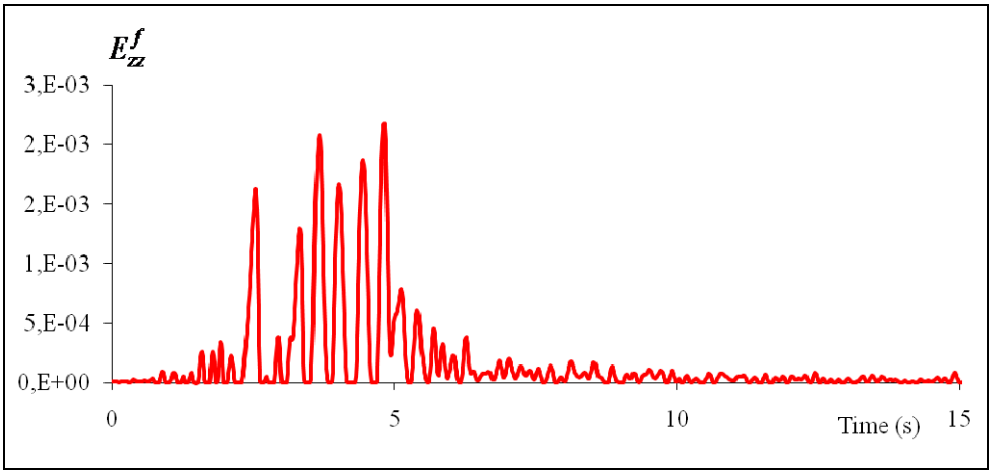

Figure 15. Fracture strain E^f_{zz} vs. time at the base of a bell chamber's pillar (node 18253).

strain tensor E^f_{zz}. A plot of the relative x-displacement of the top of the pillar with respect to the base in Figure 13 reveals a maximum values of about 0.018 m, wich corresponds to the limit value acceptable according to the Italian regulations [19] for the interstory drift of slender masonry elements (0,6% of the element's height).
Figure 16 and 17 show some parameters that can be considered representative of the tower's global dynamic response. In particular, Figure 16 shows a plot of the tower's top displacements. Figure 17 instead shows a plot of the discrete Fourier transform[1] (DFT) of the Nocera Umbra accelerogram, together with the DTF of the x – acceleration component of a node at the top of the tower for both the linear

[1] Given n real values $f_1, \ldots, f_n$, the discrete Fourier transform $f^{FT}(\varphi)$ is calculated according to the expression $f^{FT}(\varphi) = \frac{1}{\sqrt{n}} \sum_{r=1}^{n} f_r \, e^{-2\pi \, i \, (r\text{-}1)(\varphi\text{-}1)/n}$, with φ the frequency [20].

elastic and nonlinear case. The figure clearly reveals that the nonlinear case cuts the resonances on the lowest mode (about 0.7 Hz), as well as on the second mode (about 3.9 Hz), while in both cases a small amplification occurs between 2 and 3 Hz, corresponding to the strongest frequency components of the Nocera Umbra accelerogram [21].

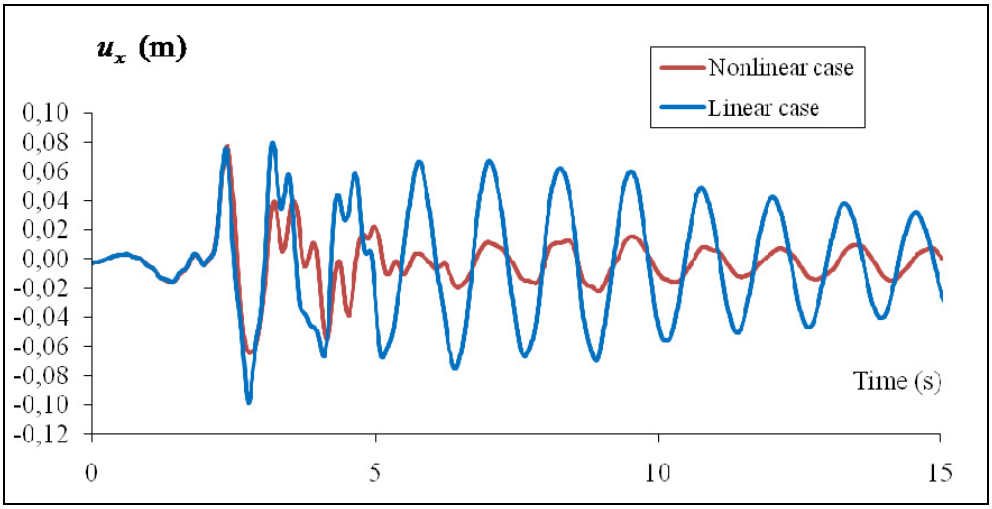

Figure 16. Relative x-displacement u_x of the top of the tower vs. time.

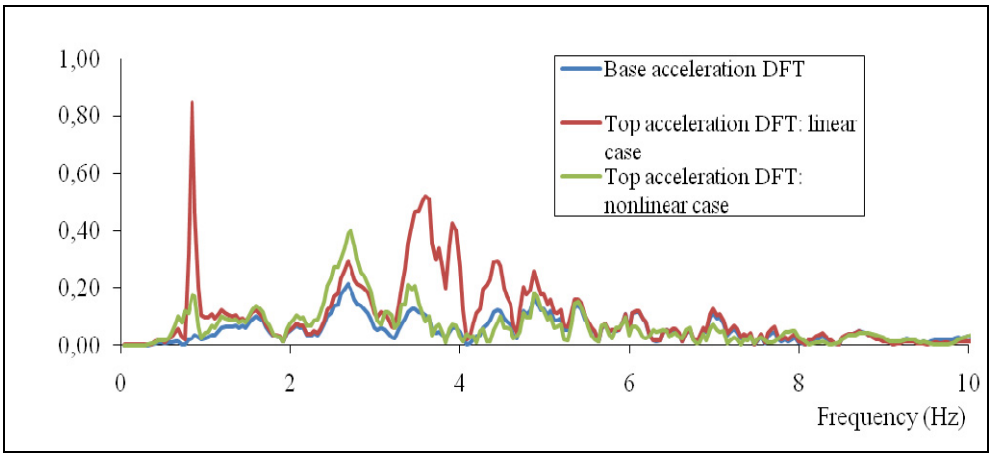

Figure 17. DFT of the Nocera Umbra accelerogram (blue line) and DFT of the *x*-acceleration calculated at node 18084 (top of the tower) for the linear case (red line) and nonlinear case (green line).

4 Conclusions

This paper presents a case study in which visual computing and computational mechanic technologies are applied in parallel to assess the vulnerability of the 13th century Rognosa tower in San Gimignano.

A 3D digital model of the tower and surrounding buildings has been generated by importing the data acquired by means of a time-of-flight laser scanner and processing them with the VC Lab software package. Then, a finite element mesh has been created and analyzed via the NOSA code, in which masonry is modelled as a nonlinear elastic material with different behavior under tensile and compressive stresses.

Good results have been achieved with regard to both the geometry acquisition and the structural modelling of the tower. However, some effort is still needed to attain tighter, more direct integration between the visual computing and the structural tools. Moreover, the NOSA code enables performing nonlinear dynamic analyses on very complex models, thereby capturing some important dynamic properties of masonry structures. However, further development is necessary in order to support more efficient, meaningful interpretations of analysis results and improve masonry damage detection using more sophisticated constitutive equations.

Acknowledgements

This research funding of the Region of Tuscany (project ST@RT - Sciences and technologies for the Tuscany Artistic, Architectural and Archaeological Heritage) is gratefully acknowledged.

References

[1] P. Cignoni, M. Callieri, M. Corsini, M. Dellepiane, F. Ganovelli, G. Ranzuglia, “MeshLab: an Open-Source Mesh Processing Tool”, Sixth Eurographics Italian Chapter Conference, 129-136, 2008.

[2] M. Callieri, P. Cignoni, F. Ganovelli, C. Montani, P. Pingi, R. Scopigno, "VCLab's Tools for 3D range data processing", 4th International Symposium on Virtual Reality, Archaeology and Intelligent Cultural Heritage (VAST2003) and First EUROGRAPHICS Workshop on Graphics and Cultural Heritage, Brighton (UK), 5-7 November 2003.

[3] K. Pulli, “Multiview registration for large datasets”. In Proc 2nd Int.l Conf. on 3D Digital Imaging and Modeling, 160–168. IEEE, 1999.

[4] W. E. Lorensen, H. E. Cline, “Marching cubes: a high resolution 3D surface construction algorithm”. In ACM Computer Graphics (SIGGRAPH 87 Proceedings),volume 21, pages 163–170, 1987.

[5] T. Lewiner, H. Lopes, A. Wilson Vieira, G. Tavares. “Efficient implementation of marching cubes’ cases with topological guarantees”. Journal of Computer Graphics, 8(2):1–15, 2003.

[6] A.R. Selby, J.M. Wilson, “The dynamics of masonry bell towers”, Computational Modelling of Masonry, Brickwork and Blockwork Structures, Edited by J. W. Bull, Saxe-Coburg Publications, 79-106, 2001.

[7] S. Ivorra S., F.J. Pallarés, “Dynamic investigation on a masonry bell tower”, Engineering Structures, 28, 660-667, 2006.

[8] M. Betti, G. Bartoli, P. Spinelli, B. Tordini, “Vulnerabilità sismica della Torre Grossa di San Gimignano”. In Atti del WorkShop WONDERmasonry 2006, Edizioni Polistampa, Firenze, 2006.
[9] A. Dogangun, R. Acar, H. Sezen, R. Livaoglu, “Investigation of dynamic response of masonry minaret structures”, Bull Earthquake Eng, 6, 505-517, 2008.
[10] S. Casolo, “A three-dimensional model for vulnerability analysis of slender medieval masonry towers”, Journal of Earthquake Engineering, 2(4), 487-512, 1998.
[11] M. Lucchesi, B. Pintucchi, “A numerical model for nonlinear dynamic analysis of slender masonry structures”, European Journal of Mechanics A/Solids, 26, 88-105, 2007.
[12] P.B. Laurenco, N. Mendes and R. Marques, “Earthquake Design and assessment of Masonry Structures: Review and Applications”. Trends in Civil and Structural Engineering Computing, pp. 77-101, Saxe-Coburg Publications, Stirlingshire, 2009.
[13] M. Lucchesi, C. Padovani, G. Pasquinelli, N. Zani, “Masonry constructions: mechanical models and numerical applications”. Lecture Notes in Applied and Computational Mechanics Vol. 39, Springer-Verlag, Berlin Heidelberg, 2008.
[14] S. Degl’Innocenti, C. Padovani, G. Pasquinelli, “Numerical methods for the dynamic analysis of masonry structures”, Structural Engineering and Mechanics, 22(1), 107-130, 2006.
[15] S. Degl’Innocenti, M. Lucchesi, C. Padovani, A. Pagni, G. Pasquinelli, N. Zani, 2007. Finite element modeling of masonry vaults. In Alphose Zingoni (ed.), Structural Engineering, Mechanics and Computation, SEMC 2007; Proc. III Int. Conf, Cape Town, South Africa, 10-12 September 2007. Millpress, The Netherlands.
[16] C. Padovani, A. Pagni and G. Pasquinelli, “Gli elementi guscio nel codice agli elementi finite NOSA”, CNUCE Report, CNR, 1998.
[17] C. Padovani, G. Pasquinelli and M. Šilhavý, "Processes in masonry bodies and the dynamical significance of collapse", Mathematics and Mechanics of Solids, 13, 573-610, 2008.
[18] R.W. Clough and J. Penzien, "Dynamics of structures", McGraw-Hill, 1975.
[19] Circolare Ministero beni e Attività Culturali 5 giugno 2007, n. 10175, “Linee Guida per la valutazione e riduzione del rischio sismico del patrimonio culturale con riferimento alle norme tecniche per le costruzioni”, 2007.
[20] S.Wolfram, The Mathematical Book, Fifth Edition, 2003, http://documents.wolfram.com/v5/TheMathematicaBook/
[21] M. Girardi, "Analytical and numerical methods for the dynamic analysis of slender masonry structures". In Atti del XIX Congresso AIMETA 2009, edited by S. Lenci, Aras Edizioni, Ancona, 2009.